# Electron-beam-induced structural degradation in two representative 2D MOFs: a ligand-dependent comparison

Pritam Banerjee[a*], Sara Talebi Deylamani[a], Shuqing Song[b], Kumar Varoon Agrawal[b], Joerg R. Jinschek[a*]

[a] *National Centre for Nano Fabrication and Characterisation (DTU Nanolab), Technical University of Denmark, Fysikvej 307, DK-2800 Kongens Lyngby, Denmark.*

[b] *Laboratory of Advanced Separations (LAS), École Polytechnique Fédérale de Lausanne (EPFL), Sion CH-1950, Switzerland.*

* Corresponding authors: pritam.nitjsr@gmail.com & jojin@dtu.dk

## Materials:

1. Zn-TCPP synthesis: The synthesis procedure was followed according to a previous study[1, 2]. $Zn(NO_3)_2 \cdot 6H_2O$ (4.5 mg, 0.015 mmol), pyrazine (0.8 mg, 0.01 mmol) and PVP (20.0 mg) were dissolved in 12 mL of the mixture of DMF and ethanol (V:V=3:1). Then ligand solution was prepared by adding TCPP (4.0 mg, 0.005 mmol) to 4 mL of the mixture of DMF and ethanol (V:V=3:1). The ligand solution was added dropwise to metal solution under stirring. After 20 minutes of mixing, the solution was sonicated for 10 min. The vial was heated to 80 °C and then kept the reaction for 16 h. The resulting purple nanosheets were washed three times with ethanol and collected by centrifuging at 7,000 r.p.m. for 10 min. Finally, the synthesized Zn-TCPP nanosheets were redispersed in ethanol.

2. $Zn_2(bim)_4$ synthesis: The $Zn_2(bim)_4$ sample was prepared according to our previously reported method[3, 4]. Graphene on a Si wafer was used as the substrate. $Zn_2(bim)_4$ films were grown by immersing the substrate in a precursor solution containing 3.12 mM $Zn^{2+}$ and 3.0 mM benzimidazole for 5 min per cycle for 10 cycles. After each cycle, residual solution at the substrate edges was gently removed using a tissue. The as-grown sample was then scraped directly onto a TEM grid for ED characterization.

## Methods:

Single-crystal ED analysis:

The indexing of the Bragg spots for the single crystals Zn-TCPP and $Zn_2(bim)_4$ sheet is performed using Crystal Maker and single-crystal software. The intensity of the Bragg spots was measured using Gatan Digital Micrograph GMS 3.5 software. The peak and background intensities were calculated by averaging 3×3 pixels centred on and surrounding the Bragg spot, respectively. The background-subtracted intensity (I) of the Bragg spot was measured by subtracting the average background intensity from the average peak intensity as a function of cumulative dose. The peak maxima ($I_m$) were measured across the ED series, and the relative intensity ($I/I_m$) of the specific Bragg plane is plotted as a function of cumulative dose. The cumulative dose corresponding to a 37% reduction in relative intensity is considered the critical dose for a specific Bragg plane.

Polycrystalline ED analysis:

The radial peak-intensity profiles of the Bragg planes of multiple Zn-TCPP sheets were determined across the ED series. The background of the Bragg peak intensity profiles of the ED series was manually fitted. The background-subtracted intensity (I) of the Bragg plane was measured by

subtracting the fitted background intensity from the peak intensity profile as a function of cumulative dose. The peak maxima ($I_m$) were measured across the ED series, and the relative intensity ($I/I_m$) of the specific Bragg plane is plotted as a function of cumulative dose. The cumulative dose corresponding to a 37% reduction in relative intensity is considered the critical dose for a specific Bragg plane.

Atomic Force Microscopy (AFM)

The thickness of Zn-TCPP nanosheets was determined by AFM using a Bruker Dimension Icon instrument operated in tapping mode under ambient conditions, employing a Tap150Al probe. Samples were prepared by drop-casting a dilute dispersion of Zn-TCPP in ethanol onto silicone substrates and allowing the solvent to evaporate at room temperature. AFM images were acquired over scan areas ranging from 2 × 2 to 8 × 8 μm² at a scan rate of 1.0 Hz. The thickness of individual flakes was extracted from height profiles taken across the edges of well-isolated sheets, where the step height between the substrate surface and the upper face of each flake was measured. Cross-sectional profiles were recorded at a minimum of five different locations per flake, and multiple flakes were analyzed to ensure statistical reliability. Image processing and height analysis were performed using Nanoscope Analysis software (Bruker).

High-Resolution Transmission Electron Microscopy (HRTEM)

High-resolution imaging was performed using a Thermo Fisher Scientific Titan transmission electron microscope equipped with a field-emission gun and operated at an accelerating voltage of 300 kV with a beam current of 0.06 nA. Samples were prepared by drop-casting a dilute dispersion of Zn-TCPP in ethanol onto lacey carbon-coated copper TEM grids (200 mesh) and allowing the solvent to evaporate under ambient conditions prior to measurement. Image acquisition and analysis were performed using Gatan Digital Micrograph software.

Figures:

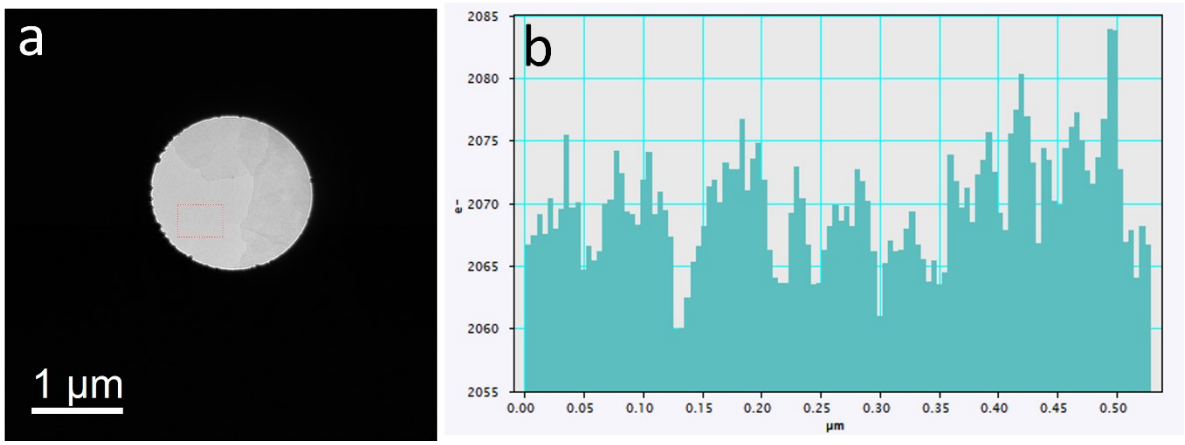


Fig. S1. Dose rate calibration (a) TEM image of the vacuum region with marked region of interest (ROI) for electron ($e^-$) count measurement. (b) The plot shows the linearly integrated electron ($e^-$) counts from the ROI region.

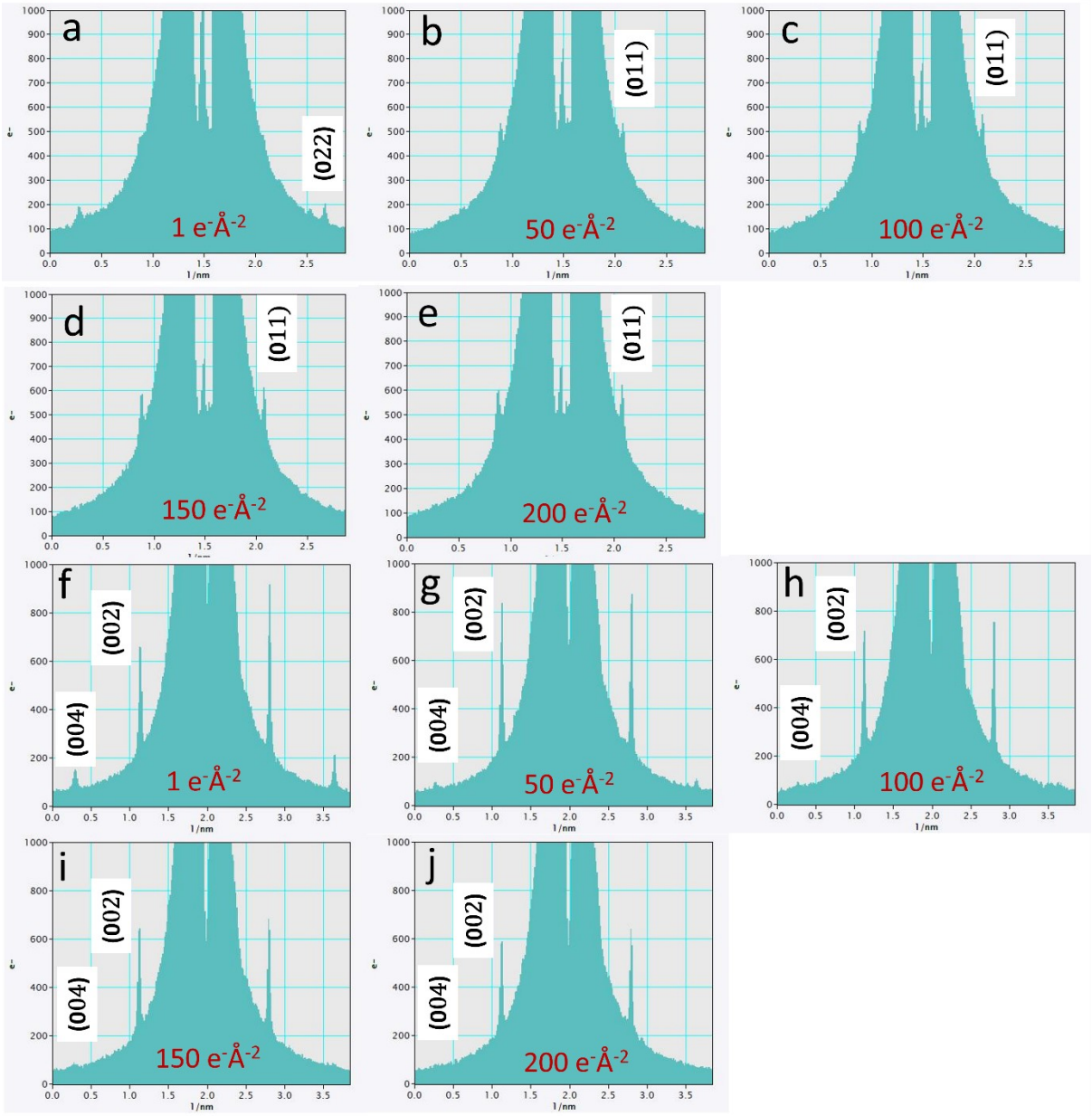


Fig. S2. (a-e) Line intensity profiles of (022) and (011) Bragg planes of Zn-TCPP sheet at cumulative doses of 1, 50, 100, 150, and 200 $e^{-}Å^{-2,}$ respectively. (f-j) Line intensity profiles of (002) and (004) Bragg planes of Zn-TCPP sheet at cumulative doses of 1, 50, 100, 150, and 200 $e^{-}Å^{-2}$, respectively.

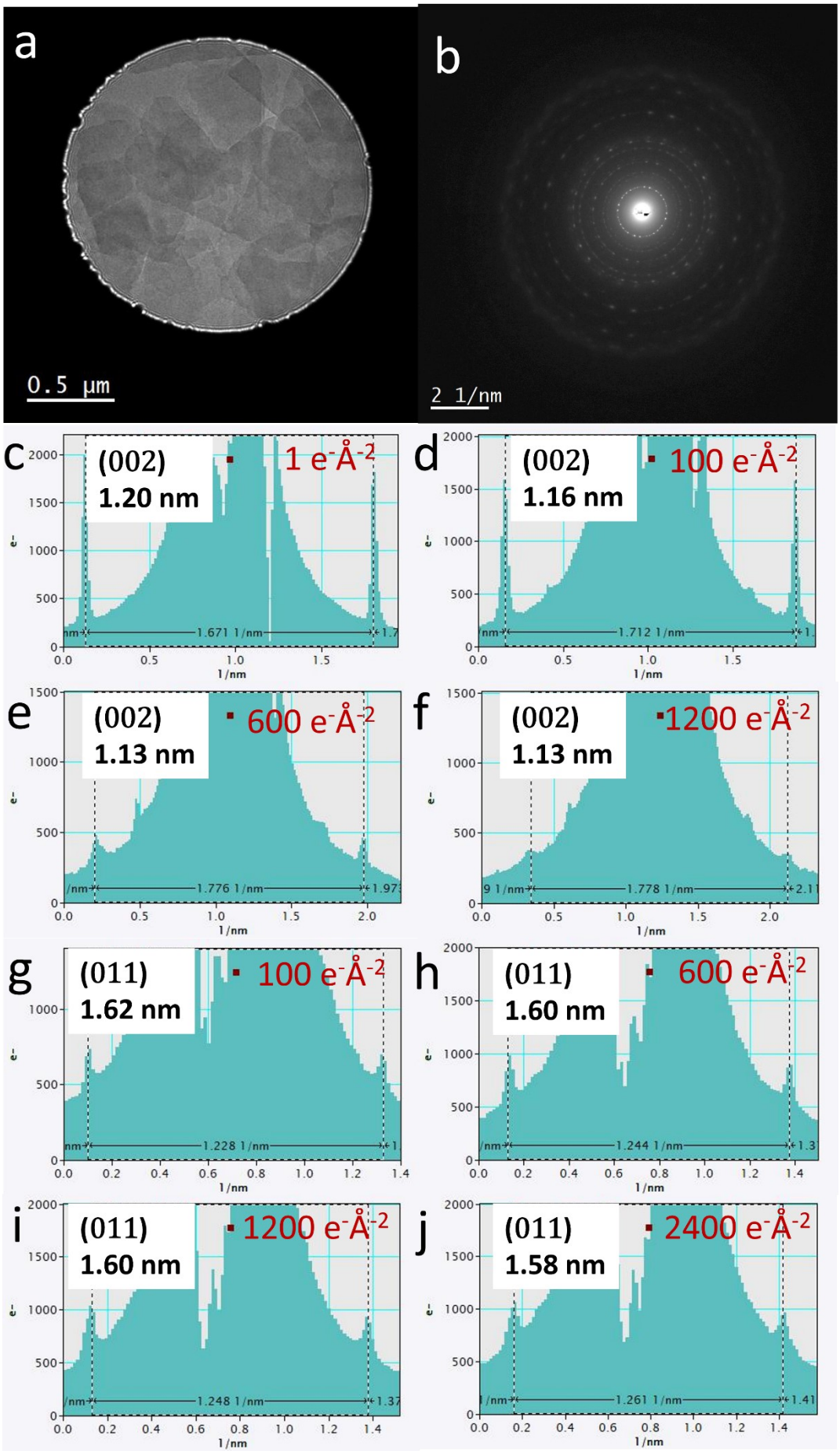
a
0.5 µm
b
2 1/nm
c
(002)
1.20 nm
1 e-Å-2
1.671 1/nm
d
(002)
1.16 nm
100 e-Å-2
1.712 1/nm
e
(002)
1.13 nm
600 e-Å-2
1.776 1/nm
f
(002)
1.13 nm
1200 e-Å-2
1.778 1/nm
g
(011)
1.62 nm
100 e-Å-2
1.228 1/nm
h
(011)
1.60 nm
600 e-Å-2
1.244 1/nm
i
(011)
1.60 nm
1200 e-Å-2
1.248 1/nm
j
(011)
1.58 nm
2400 e-Å-2
1.261 1/nm
e-
1/nm

Fig. S3. (a, b) TEM image of multiple Zn-TCPP sheets and corresponding ED ring pattern. (c-f) Line intensity profile of (020) Bragg plane at cumulative doses of 1, 100, 600, and 2400 $e^{-}Å^{-2}$, respectively. (g-j) Line intensity profile of (011) Bragg plane at cumulative doses of 1, 100, 600, and 2400 $e^{-}Å^{-2}$, respectively.

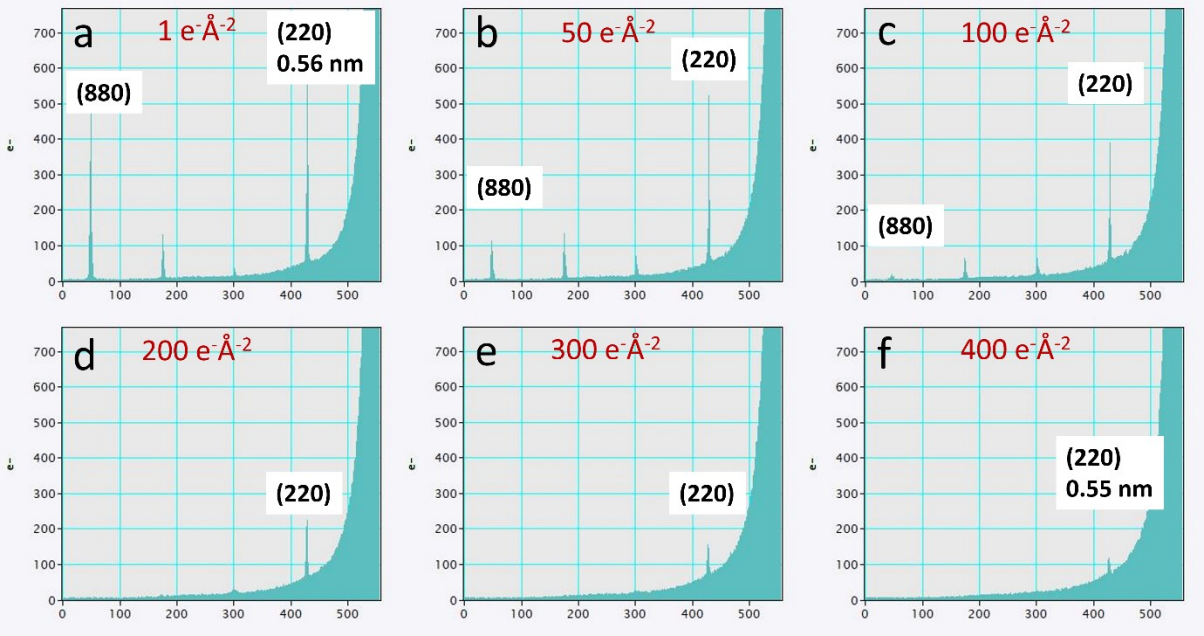


Fig. S4. (a-f) Line intensity profiles of (220) and (880) Bragg planes of $Zn_2(bim)_4$ sheet at cumulative doses of 1, 50, 100, 200, 300, and 400 $e^{-}Å^{-2}$, respectively.

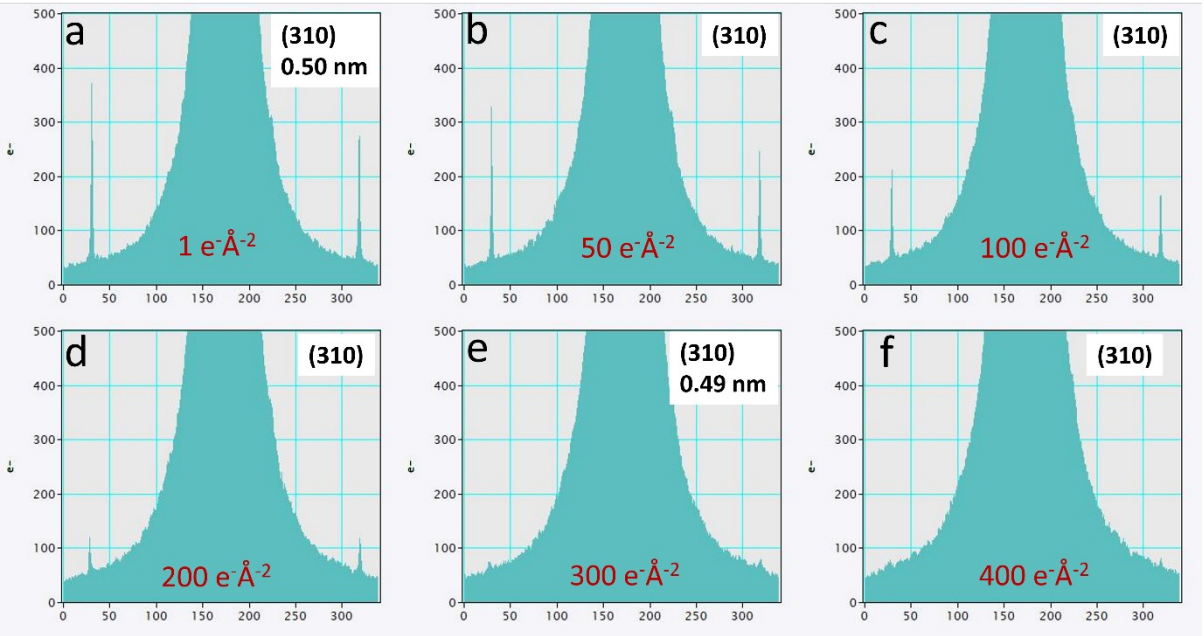

Fig. S5. (a-f) Line intensity profiles of (310) Bragg plane of $Zn_2(bim)_4$ sheet at cumulative doses of 1, 50, 100, 200, 300, and 400 $e^-Å^{-2}$, respectively.

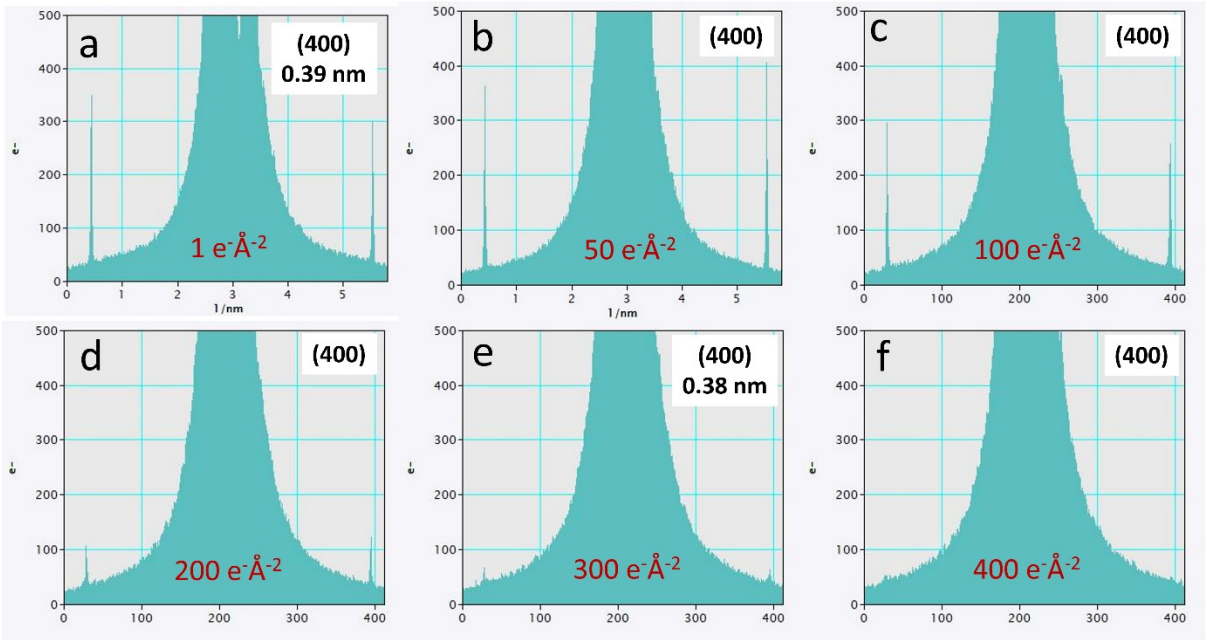


Fig. S6. (a-f) Line intensity profiles of (400) Bragg plane of $Zn_2(bim)_4$ sheet at cumulative doses of 1, 50, 100, 200, 300, and 400 $e^-Å^{-2}$, respectively.

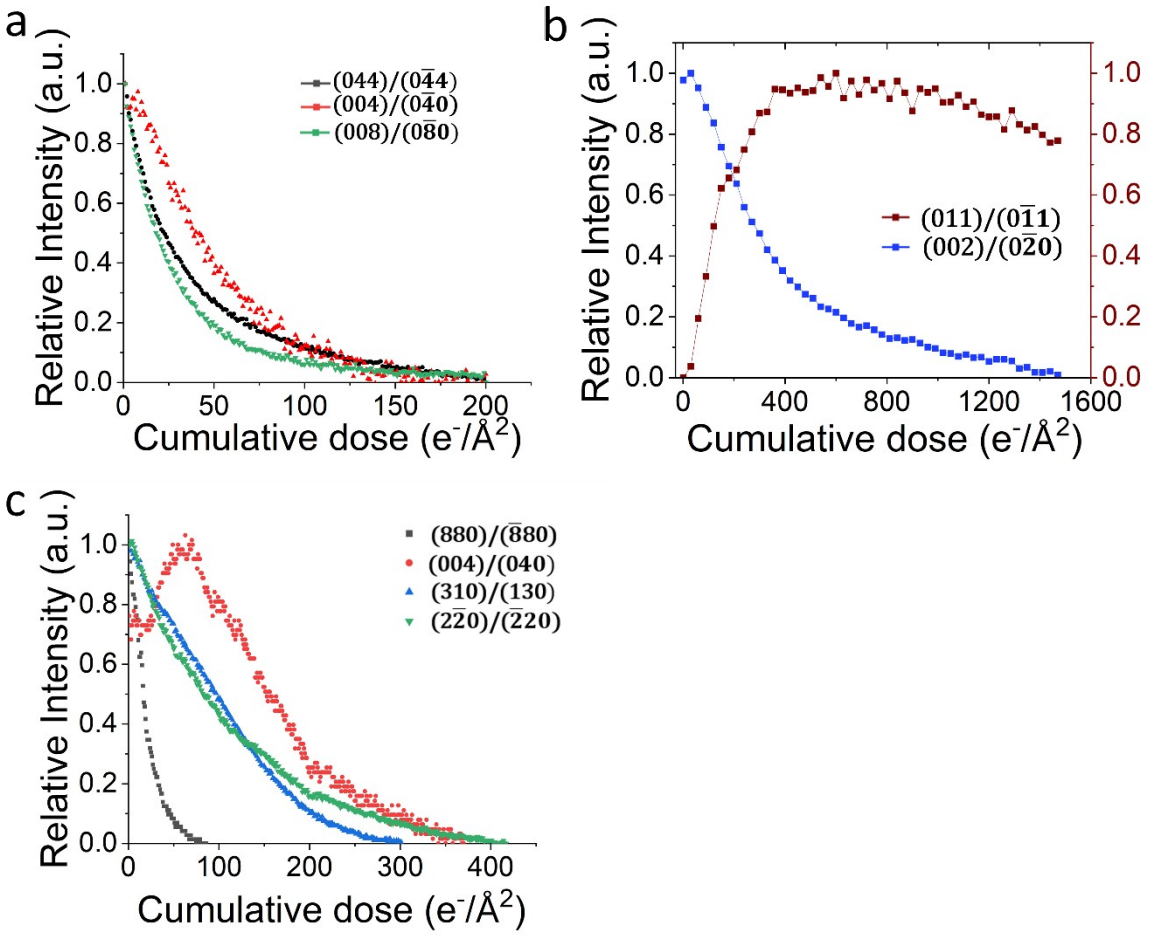


Fig. S7. (a) Relative intensities of Bragg planes (004)/(0$\bar{4}$0), (044)/(0$\bar{4}$4), and (008)/(0$\bar{8}$0), respectively, of multiple Zn-TCPP 2D sheets (dataset 2) as a function of cumulative dose. (b) Relative intensities of (002)/(0$\bar{2}$0) and (011)/(0$\bar{1}$1) Bragg planes, respectively, of multiple Zn-TCPP 2D sheets as a function of cumulative dose up to 1600 e$^-$Å$^{-2}$. (c) Relative intensities of Bragg planes (880)/($\bar{8}$80), (2$\bar{2}$0)/($\bar{2}$20), (310)/(130), and (004)/(040), respectively, of $Zn_2(bim)_4$ sheet (dataset 2) as a function of cumulative dose.

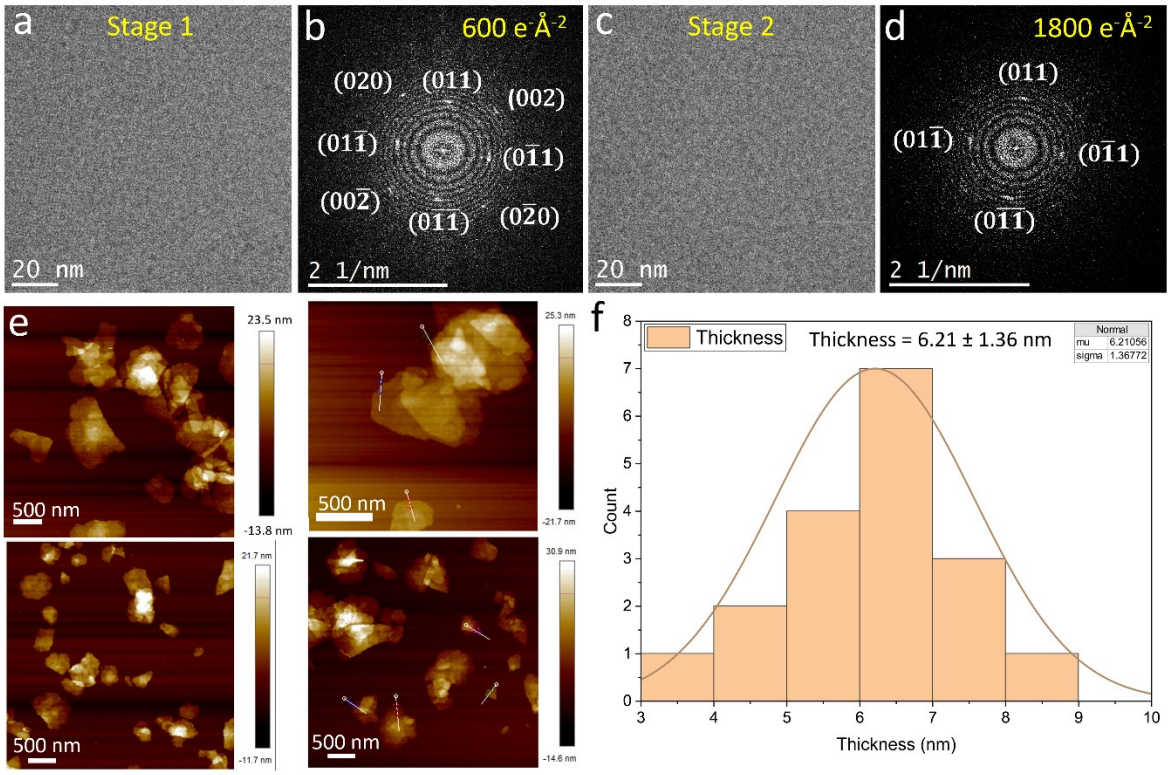


Fig. S8. (a, b) HRTEM lattice image of Zn-TCPP MOF at a cumulative electron dose of around 600 $e^{-}Å^{-2}$ and corresponding fast fourier transform (FFT) image, respectively. (c, d) HRTEM lattice image of Zn-TCPP MOF at a cumulative electron dose of around 1800 $e^{-}Å^{-2}$ and corresponding FFT image, respectively. (e, f) Atomic force microscopy images of Zn-TCPP MOF and the corresponding histogram representing the thickness profiles.

Video_S1: ED series of a single Zn-TCPP sheet (dataset 1) with a cumulative electron dose ranging from 1 to 200 $e^{-}Å^{-2}$.

Video_S2: ED series of multiple Zn-TCPP sheets (dataset 1) (ring pattern) with a cumulative electron dose ranging from 1 to 2400 $e^{-}Å^{-2}$.

Video_S3: ED series of a single $Zn_2(bim)_4$ sheet (dataset 1) with a cumulative electron dose ranging from 1 to 480 $e^{-}Å^{-2}$.

Video_S4: ED series of a single Zn-TCPP sheet (dataset 2) with a cumulative electron dose ranging from 1 to 300 $e^{-}Å^{-2}$.

Video_S5: ED series of multiple Zn-TCPP sheets (dataset 2) (ring pattern) with a cumulative electron dose ranging from 1 to 1600 $e^{-}Å^{-2}$.

Video_S6: ED series of a single $Zn_2(bim)_4$ sheet (dataset 2) with a cumulative electron dose ranging from 1 to 480 $e^{-}Å^{-2}$.

Reference:


(1) Zhao, M.; Wang, Y.; Ma, Q.; Huang, Y.; Zhang, X.; Ping, J.; Zhang, Z.; Lu, Q.; Yu, Y.; Xu, H.; Zhao, Y.; Zhang, H. Ultrathin 2D Metal–Organic Framework Nanosheets. *Adv. Mater.* **2015**, *27* (45), 7372–7378. https://doi.org/10.1002/adma.201503648.

(2) Zhu, Z.-H.; Liu, Y.; Song, C.; Hu, Y.; Feng, G.; Tang, B. Z. Porphyrin-Based Two-Dimensional Layered Metal–Organic Framework with Sono-/Photocatalytic Activity for Water Decontamination. *ACS Nano* **2022**, *16* (1), 1346–1357. https://doi.org/10.1021/acsnano.1c09301.

(3) Song, S.; Liu, Q.; Swathilakshmi, S.; Chi, H.-Y.; Zhou, Z.; Goswami, R.; Chernyshov, D.; Agrawal, K. V. High-Performance H 2 /CO 2 Separation from 4-Nm-Thick Oriented Zn 2 (Benzimidazole) 4 Films. *Sci. Adv.* **2024**, *10* (50), 1–11. https://doi.org/10.1126/sciadv.ads6315.

(4) Song, S.; Kocaman, C.; Baisil, A.; Hao, J.; Wang, S.; Agrawal, K. V. Uniform In-Plane Growth of Large-Area Ultrathin Zn 2 (Benzimidazole) 4 Membrane. *Adv. Funct. Mater.* **2026**, *36* (11). https://doi.org/10.1002/adfm.202525243.